Maria Sklodowska-Curie Actions (MSCA)
Innovative Training Networks (ITN)
H2020-MSCA-ITN-2018
Grant number 813137

Project number 813137

URBASIS-EU
New challenges for Urban Engineering Seismology

DELIVERABLE

Work Package: WP1
Number: D1.4 – Ground-Motion modelling as an Image processing task. Integration of new data and associated uncertainty reduction.

Authors:	**Sunny, Jaleena**	(UoL)
Co-authors:	Cotton, Fabrice	(GFZ)
	Lilienkamp Henning	(GFZ)

Reviewer	Edwards, Ben	(UoL)
Approval	Management Board	
Status	Final Version	
Dissemination level	Public	
Delivery deadline	31.07.2022	
Submission date	31.07.2022	
Intranet path	https://urbasis-eu.osug.fr/Scientific-Reports-157	

Contents

1 Abstract

To better understand the effect and influence of spatial density of ground motion predictions, we attempted to combine data from multiple seismic networks from the same region and compare intensity predictions with and without new seismological networks. The U-Net neural network architecture is used as a ground motion model that predicts the mean and standard deviation of a target intensity measure (IM, PGA) in the form of maps. The U-Net can interpolate the intensity measures between the observation points inherently and we here try to analyse the effect of spatial density in this interpolation by using multiple networks. Kanto basin in Japan is selected for this study due to the availability of dense seismic networks within the basin and we integrated the KIK-net and the MeSO-net networks within the basin for this study. The results show that the errors and the uncertainty levels between the predictions and the observations at the interpolated sites slightly decreased after adding an additional network for the training process, but the statistical significance is questionable. However, more networks or more observations per station are required to be integrated and trained within the same region to analyse and validate our results.

2 Introduction

Over the last few decades, a large number of ground-motion models (GMMs) have been developed for use in seismic hazard and risk applications all over the world. GMMs define the ground motion field in terms of earthquake source characteristics (e.g., magnitude, fault mechanism), wave propagation (e.g., epicentral distance), and site effects (e.g., site class or $VS30$) to predict specific intensity measures (IM). For various tectonic regions, tens or even hundreds of candidate models are available due to the intricacy of the earthquake process, wave propagation, and site effects; examples can be found in Douglas (2020). These models represent the distribution of ground-motion in terms median intensity measure and its standard deviation (Strasser et al. 2009).

The U-Net neural network architecture has been used recently as a ground motion model that predicts the mean and standard deviation of a target intensity measure (IM, PGA) in the form of maps (Lilienkamp et al. 2022).The U-Net, it learns the relationship between predictive parameters and target parameters using a large number of instances that are presented to train the neural network, just like all supervised learning techniques. In ground-motion modelling, the target parameter is a ground-motion IM, which may be deduced from predictive factors such as the moment magnitude M_w and the hypocentral distance r_{hyp}. The U-Net neural network architecture has been used recently as a ground motion model that predicts the mean and standard deviation of a target intensity measure (IM, PGA) in the form of maps (Lilienkamp et al. 2022). The U-Net can interpolate the intensity measures between the observation points inherently and we here try to analyze the effect of spatial density of observation points in this interpolation by using multiple seismological networks (e.g. MeSO-NET).

To better understand the effect and influence of arrays spatial density on ground motion predictions, we attempted to combine data from multiple seismological networks from the same region and compare intensity predictions with and without new seismological stations.The relative surface fault motion for recording stations situated on either side of a causative fault, soil liquefaction, landslides, and the general transmission of the waves from the source through the various earth strata to the ground surface can all contribute to the spatial variability in seismic ground motions (Zerva & Zervas 2002). This architecture's inherent capacity to process data in the form of 2D arrays (maps) makes it particularly appealing for ground-motion modeling, as it allows for native operations on map data, which preserves the underlying spatial distribution of ground-motion observations (Lilienkamp et al. 2022). This visualization method provides a clear picture of how spatial density of observation points affects ground motion predictions. This spatial variation of seismic ground motions has started being analyzed after the installation of these kinds of dense instrument arrays. The sensors used for these arrays are costly and also time-consuming, hence studies are required to really understand the effect of these arrays and to find an optimal array that minimises the error in model predictions. In this study, we focus on the effect of spatial density of the stations in the intensity predictions and the associated uncertainties by integrating data from different seismological networks.

In this report, we use the U-net architecture to understand the relation between the IM (here PGA) and predictive parameters in the Kanto basin using a subset of the Kiban–Kyoshin (KiK-net) dataset. We then look at how integrating two datasets from the same region (Kanto Basin) - the KiK-net and the highly dense Metropolitan Seismic Observation network (MeSO-net), affects the interpolation of IMs and their associated uncertainties between the observation points. Here we work with the PGA values while the original work of (Lilienkamp et al. 2022) focused and tested only for SA(T=1s).

3 Data Used

Kanto basin in Japan is selected for this specific study due to the high-density seismic networks available within the basin. The basin has KiK- et stations, MeSO-net stations (Sakai & Hirata 2009), K-net stations (National Research Institute for Earth Science and Disaster Resilience, 2019) and some QuakeSaver devices are also installed within some buildings in the region.

We are primarily interested in determining and analyzing the difference in the uncertainty in U-Net's interpolation of intensity measures between station locations when data from numerous networks is used instead of a single network, hence, the goal of our study necessitates the use of high-density networks of this type. We focus on two networks in this report, i.e, KiK-net and MeSO-net as shown in Figure 1. Both KiK-net and MeSO-net are operated by National Research Institute for Earth Science and Disaster Resilience, NIED (2019).

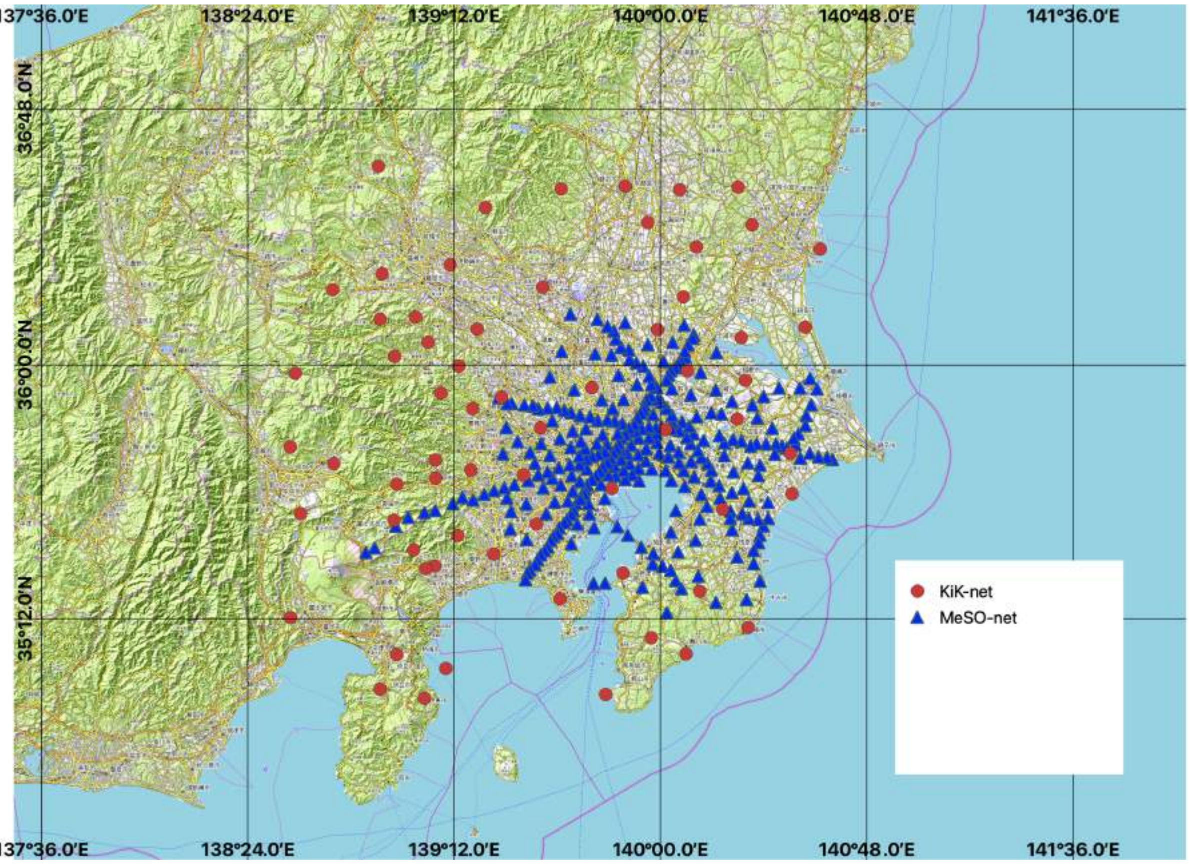

Figure 1: *KiK-net and MeSO-net station coverage in the Kanto Basin. Blue triangles indicate the MeSO-net locations (highly dense) and the red circles are the KiK-net station locations.*

3.1 KiK-net dataset

KiK-net consists of pairs of strong-motion seismographs installed in a borehole and on the ground surface. Here, we used exactly the same dataset given by Bahrampouri et al. (2021) comprising both surface and borehole sensors. We downloaded the processed data by Bahrampouri et al. (2021). The database utilized in this study comprises all earthquakes with a magnitude greater than three that were recorded on the KiK-net website between 1996 and the end of 2017 and used by Bahrampouri et al. (2021), Lilienkamp et al. (2022). We used 46,191 records from 2864 events recorded at 65 different stations. The selected KiK-net stations have an average inter-station distance of about 94 km. As our target intensity, we used the geometric mean of the PGA values. The distribution of the dataset is given in Figure 2.

3.2 MeSO-net dataset

MeSO-net is made up of around 300 observation stations in the Tokyo metropolitan region, as illustrated in Figure 1 (blue triangles). These stations are made up of five dense linear arrays spaced around 2 to 3 km apart and a sparser distribution with a radius of about 80 km spaced roughly 4 to 10 km apart. This network is highly dense compared to the inter-station distance of KiK-net stations. MeSO-net stations (three-component accelerometer) are located at the bottom of 20 m deep boreholes. This data is converted to correspond to the intensity at the ground surface according to Aoi et al. (2021) by adding 0.5 to log(PGA) at all stations at all stations (accounting for the free surface factor).

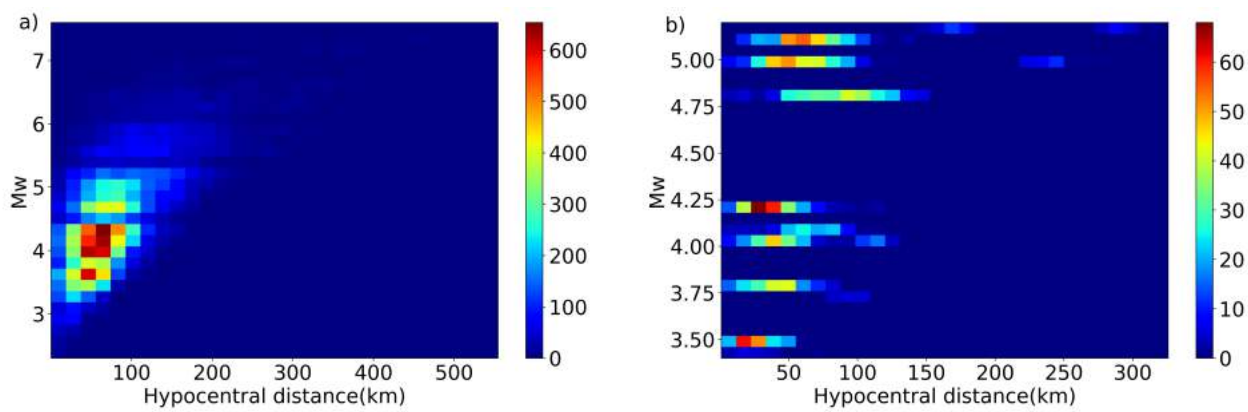

Figure 2: *Data from Kanto basin used for this study. Hit counts computed for the data distribution, dividing the distance range into 20 equally spaced bins over the hypocentral distance and the moment magnitude (Mw). a) KiK-net dataset b) MeSO-net dataset.*

The MeSO-Net waveform data is downloaded from the National Research Institute for Earth Science and Disaster Resilience (NIED) website. The website provides the data from 2021 and 2022. A total of 1921 recordings are obtained from 19 events recorded at 300 different stations in the Kanto Basin. Figure 2 depicts the data distribution of both networks - the KiK-net and the MeSO-net. Data used from MeSO-net for this study is only available from a limited time period.

4 Methodology

4.1 The U-net architecture

The U-net neural network architecture (Ronneberger et al. 2015) is the central component of our methodology, as it can offer us with a fully non-ergodic and data-driven GMM. Lilienkamp et al. (2022) introduced this to the ground motion modelling area, and the paper tests the U-net as a GMM and explains how it can work as a GMM. Figure 2 illustrates this. The input parameters are the nine maps shown in the figure, i.e, the latitude and longitude of the event, the depth, magnitude, the coordinates of each pixel in the input layer (572 $\times$ 572 pixels), the hypocentral distance and the depth to seismic bedrock. The output will be the mean, $\hat{y}$ and variance, σ^2 of the IM. The valid convolution operations reduces the resolution of the output features is to 388 $\times$ 388 compared to that of the input features. Through a series of instances and iterations, the U-net algorithm learns the link between the input parameters and the output. Detailed information on the neural networks can be found in LeCun et al. (2015). The U-net is particularly useful for ground motion modelling since it is designed to process data in the form of 2D arrays, or maps. The U-Net's predictive parameters are provided in the form of a stack of maps spanning a predefined area, and the U-Net is trained to provide estimates of the target IM's mean and variance. The negative log-likelihood is considered as the model error or the loss between the model outputs and the observations for an event with N observations. The loss is iteratively minimized using the gradient descent algorithm Adam (Da 2014), with the gradient effectively implemented using backpropagation (Rumelhart et al. 1986).

After one cycle (epoch) of training using all of the training data, the neural network's training is tested using the validation dataset. After a given number of epochs, the loss on the validation dataset does not decrease any further, indicating that the training is complete and the U-Net may now be used as a GMM. Instead of point-wise observations,

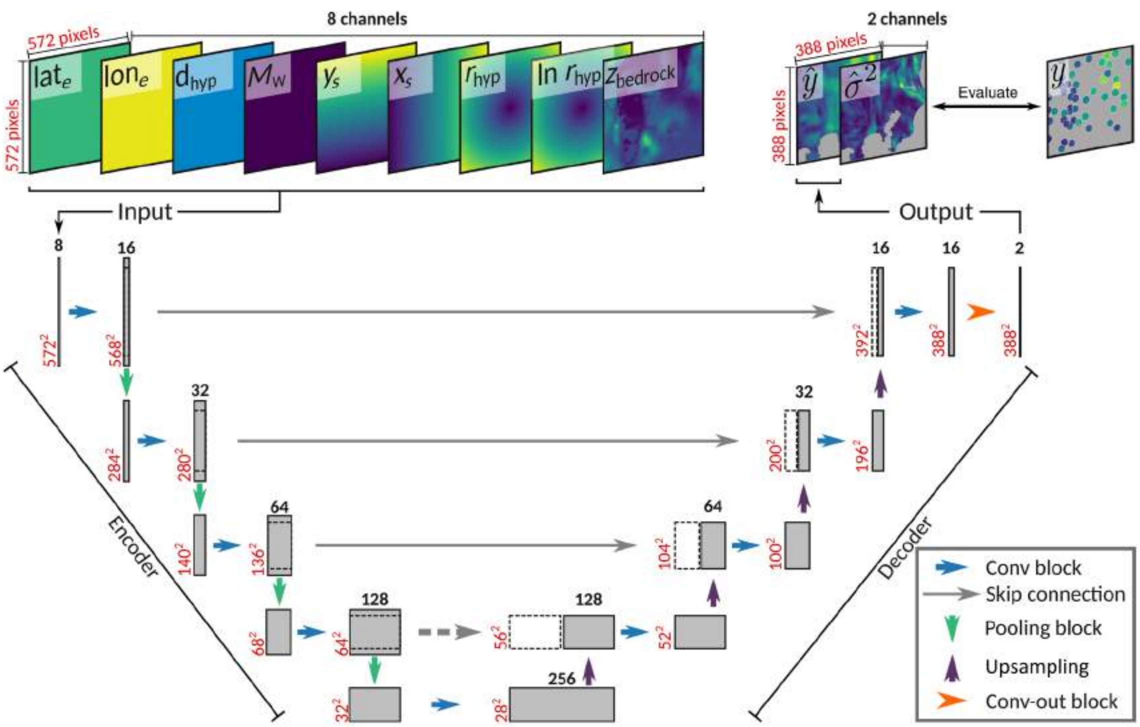

Figure 3: *This study's U-Net architecture [Figure from Lilienkamp et al. (2022)]. The U-Net receives the predictive parameters for a single earthquake as input in the form of a stack of maps. The input is processed, and the intensity measure (IM) mean $\hat{y}$ and variance $\hat{\sigma}^2$ estimators are provided as output. Lat$_e$, lon$_e$, and d$_{hyp}$ are the latitude, longitude, and depth of the event hypocenter, respectively. Mw is the moment magnitude, xs and ys are the coordinates of each pixel in the input layer, rhyp is the hypocentral distance, and $z_b$edrock is the depth to seismic bedrock. This figure is described in more detail in (Lilienkamp et al. 2022). This figure is based on the first figure of Ronneberger et al. (2015).*

the U-net predictions are continuous maps. This means that the loss function is generated first at sites where actual observations are available, and then the U-Net interpolates the learned attenuation relation from those locations. The data was separated into training and validation events using the same training technique as (Lilienkamp et al. 2022), i.e.,

- The data were divided into training and validation events.All events occurring up to 2015 are used for training, while those occurring 2015 and onwards are considered validation events.

- Stations are divided into a number of chunks at random (N_{chu}) - for each station chunk, one U-net is trained (the selected station chunk is excluded from training in order to be used for validation after training).

- The U-net is run N_{init} times to quantify the variability caused by random coefficient initialization. The final predictions for the mean and variance of the target IM for the event e ($\hat{Y_e}$ and the $\hat{\Sigma}_e$,respectively), are obtained by ensemble averaging the mean and variance predictions of the individual U-Nets ($\hat{y_e}^{ij}$ and the $\hat{\sigma_e}^{ij}$,respectively). The total number of U-Nets will be, $N_U = N_{chu} * N_{init}$ and the mean and variance of the final predicted IM according to the law of total expectation and the law of total variance (Blitzstein & Hwang 2015) for an event will be

$$\hat{Y_e} = 1/N_U \sum_{i=1}^{N_{chu}} \sum_{j=1}^{N_{init}} \hat{y_e}^{ij} \tag{1}$$

$$\hat{\Sigma}_e^2 = 1/N_U \sum_{i=1}^{N_{chu}} \sum_{j=1}^{N_{init}} [\hat{\sigma_e}^{ij^2} + \hat{y_e}^{ij^2}] - \hat{Y}_e^2 \tag{2}$$

The U-Net learns the site amplification as a function of the coordinates of the station location, source-location specific variability from the event latitude and longitude, and path-specific amplification from the coordinates of each pixel and from the latitude and longitude of the events. We initially analyzed the U-net findings using only the KiK-net dataset, then trained the U-net using both the KiK-net and MeSO-net datasets to see how the results differ in terms of increasing the number of observation sites between the existing ones (the KiK-net stations).

4.2 U-Net training with different seismological networks - Kanto Basin

We started (the first stage) of the U-Net training with the KiK-net strong-motion dataset by (Bahrampouri et al. 2021) for peak ground acceleration (PGA) measurements. All events occurring up to 2015 are used for training, while those occurring 2015 and onwards are considered validation events. The 65 stations are separated into 5 chunks, with each chunk receiving a random selection of the stations and 10 random initializations. We proceed with the inclusion of the MeSO-net dataset after obtaining the predicted PGA values with the KiK-net dataset. We use both the KiK-net and MeSO-net recordings for the training in this stage. For the training phase, both the events occurring before 2015 (only KiK-net) and after 2020 (only MeSO-net events) are evaluated. The validation events are set as the same sets we used in the first step in order to understand the changes after adding a new dense network (MeSO-net) with the KiK-net data in training process, i.e, the same KIK-net station chunks are used for validation of interpolated IM values. A summary of this is shown in the flowchart.(Figure 4)

5 Results and Discussion

5.1 Interpolation Quality

We first analyse the effect in the interpolation of IMs when arrays of stations (MeSO-net) are integrated to the KiK-net dataset in the same region, Kanto basin. As we have discussed earlier the U-net automatically interpolates the learned relation from the observation locations across the output area and we study the quality of this interpolation using the partial ensemble estimators, $\hat{\mathcal{Y}}^i$, for which the ith station chunk was not used during training. Averaging over the subsets of U-Nets that share the same ith station validation chunk yields partial ensemble estimators. Lilienkamp et al. (2022) evaluated and classified these partial ensemble estimators in four different ways to understand the performance of U-Net at the interpolated sites and we use the same technique to assess the effect of spatial density in the interpolation. The four different categories are (1) training events recorded on training stations, (2) validation events recorded on training stations, (3) training events recorded on validation stations, and (4) validation events recorded on validation stations. We average the root mean square error (rmse) between the observations and predictions (Ln) over the five station chunks $\hat{\mathcal{Y}}^i$. The average of the rmse values using only the KiK-net

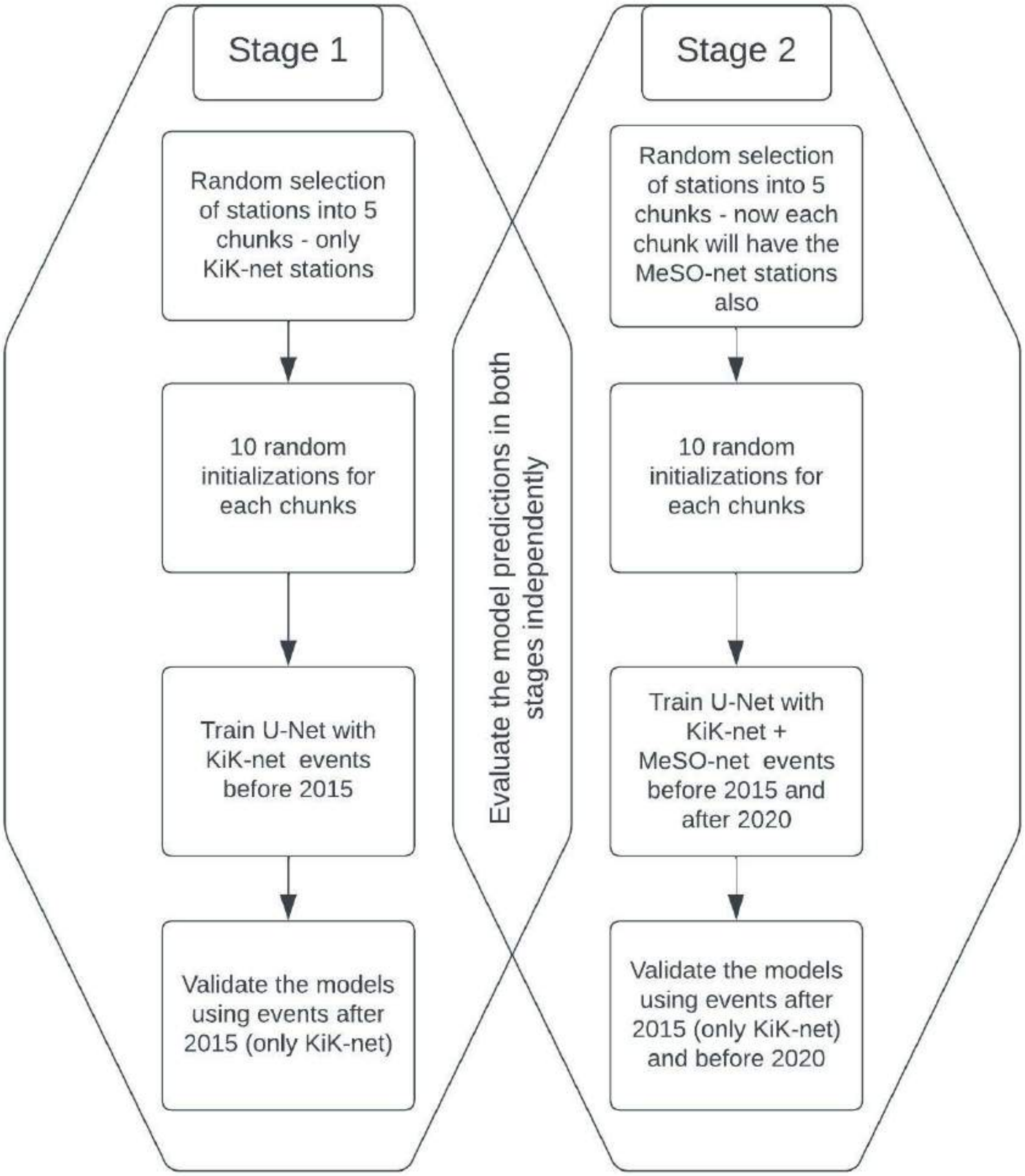

Figure 4: *Flowchart describing the process used in this study.*

stations is given in Table 1. The rmse values are larger when using the validation stations, as seen in the table, because these predictions from the validation stations have additional errors owing to interpolation. The training events and the training stations will have the smallest rmse values as those observations are the ones used for training.

Table 1: *Average Root Mean Square Errors ± 1 Standard Deviation between Observations and Predictions of the Five Partial Ensemble Estimators using only KiK-net.*

Configuration	**Rmse**
Training stations/training events	0.432 ± 0.007
Training stations/Validation events	0.496 ± 0.005
Validation stations/training events	0.871 ± 0.104
Validation stations/validation events	0.854 ± 0.090

Table 2: *Average Root Mean Square Errors ± 1 Standard Deviation between Observations and Predictions of the Five Partial Ensemble Estimators using both KiKnet and MeSO-net.*

Configuration	**Rmse**
Training stations/training events	0.429 ± 0.007
Training stations/Validation events	0.494 ± 0.005
Validation stations/training events	0.865 ± 0.086
Validation stations/validation events	0.841 ± 0.080

The rmses in Ln units are then analyzed using both the KiK-net and MeSO-net stations to see how integrating more stations affects the results. The validation stations rmses with and without the MeSO-net stations are of particular interest because they are the predictions with the interpolation error. The average of the rmses between the observations and predictions over the five $\hat{\mathcal{Y}}^i$ using both the networks is given in Table 2. As shown in the table the rmse values decreased in all the four configurations. The change of rmses are within the standard deviation provided in the tables for all the four combinations, which may provide the idea that the changes are not that significant. Due to the small number of MeSO-net records compared to KIK-net records, the influence on training the neural network is relatively small. Thus, while the number of records is small, the MeSO-net network is actually predestined to improve the quality of interpolated values in this region. We may observe more significant changes in the validation stations on validation events combination by using a more temporal dense network, eg.the Kyoshin Network (K-net), (NIED 2019).

We also try to understand the effect on the uncertainty in prediction when another seismological networks are integrated to the training dataset. Lilienkamp et al. (2022) used $\hat{\Sigma}$ (given in equation 2) as a proxy for the scatter in observations at station locations, as it is what we learn with the neural network, and it is supposed to have learned the scatter in observations and verified its reliability by comparing the distribution of the standardized residuals, $\tilde{\Delta}$, with the standard normal distribution. The residuals are standardized by dividing each individual residual by its predicted standard deviation, $\hat{\Sigma}$. We calculated the $\tilde{\Delta}$ achieved using only the KiK-net data and also together with the MeSO-net dataset for training. Once this is achieved we compare it with the target normal distribution to analyse the difference in both distributions (Figure 5). We get a similar standard deviation of $\tilde{\Delta}$ in both cases, i.e around 14-15 % decrease than the targeted value. Since, we standardized

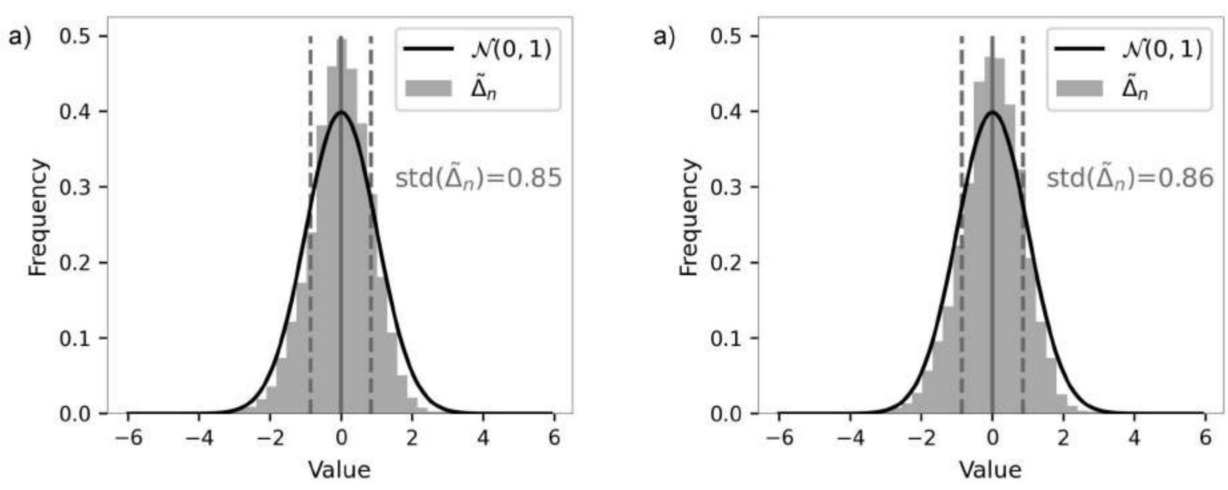

Figure 5: *Comparison of the distribution of standardized residuals with the targeted standard normal distribution. Solid and dashed vertical lines indicate the empirical mean and standard deviation (std) of standardized residual, $\tilde{\Delta}$ respectively. a) Training with only KiK-net b) Training with both KiK-net and MeSO-net dataset.*

the residuals by dividing it by the $\hat{\Sigma}$, this standard deviation of 0.86 corresponds to an overestimation of the uncertainty in predictions.

We calculate the $\hat{\Delta}$ distribution between all observations from both training and validation events with respect to the partial ensemble estimators discussed above. All the four combinations are analysed with respect to the standard Gaussian distribution as shown in Figure 5 and 6.

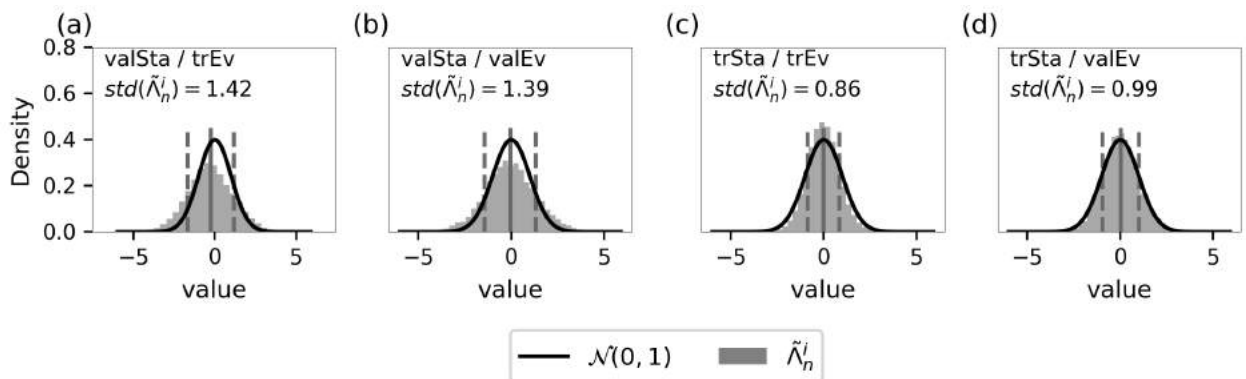

Figure 6: *Comparison of the distribution of the standardized residuals with the targeted standard Gaussian distribution for the partial ensemble estimators in all four configurations using the KiK-net dataset.*

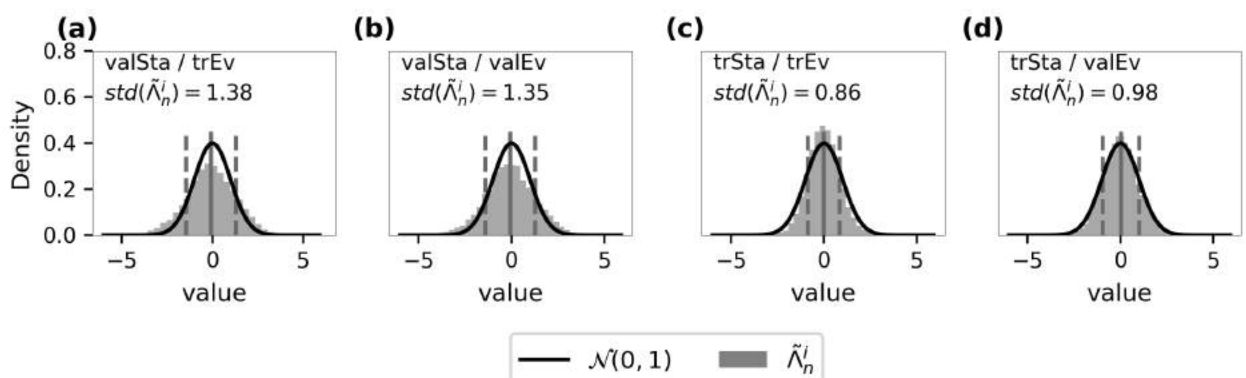

Figure 7: *Comparison of the distribution of the standardized residuals with the targeted standard Gaussian distribution for the partial ensemble estimators in all four configurations using both the KiK-net and MeSO-net dataset.*

The panels (c) and (d) in both figures gives the closest fit to the standard normal distribution and hence, we can understand that the predictive uncertainty at the training stations are reliable. But while considering the other two panels of both figures, underestimation of the predictive uncertainty is quite significant - as both are much higher than 1 (around 40%). However, the overestimation seems to decrease when an additional network is integrated to the KiK-net dataset. The standard deviation of the validation stations on validation events decreased from 1.39 to 1.35 and the validation stations on training events moved closer to 1 when MeSO-net is added to the U-Net training. These results indicate that the increase in spatial density may contribute to a slight decrease in the underestimation of the predicted standard deviation in the interpolated sites.

5.2 Site amplification

We also analysed the effect of a spatially dense seismological network in the site amplification learned by the U-net architecture. The site specific effects are calculated by training another GMM without using the predictive parameters x_S, y_s and $z_{bedrock}$. We then approximate the site amplification $\hat{Amps}$ learned by subtracting the GMM predictions with and without the site specific predictive parameters. This will provide us with the site amplification maps shown in Figure 7.

The maps are plotted for the models trained with only KiK-net and also trained with both KiK-net and MeSO-net. Both the maps behave very similar to each other and there is no significant effect on adding more station data. This may again lead to the fact that both spatially and temporally dense networks are required in understanding the detail and reliable effects.

When the map (only using KiK-net) is compared with the amplification maps at SA 1s (Figure 8), significant deamplification can be observed. This may be because of the use of $z_{bedrock}$ as the predictive parameter for site and hence, this may indicate that the sediments in the basin are damping high frequencies. More studies are required to understand the difference in site amplification in different frequencies.

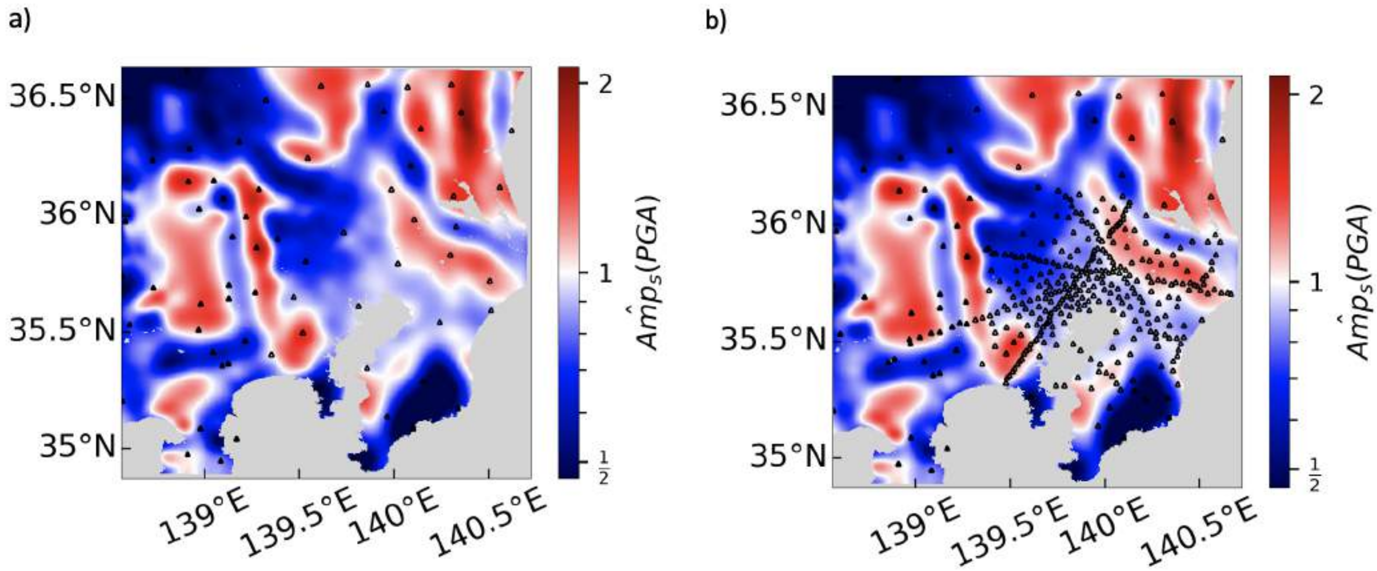

Figure 8: *Site amplication estimation of PGA in the Kanto basin approximated from averaged mean predictions. a) KiK-net b) KiK-net + MeSO-net. The black triangles indicate the station locations*

6 Conclusion and Future work

The importance of spatial density in predicting ground motion IMs using the method developed recently by Lilienkamp et al. (2022) for several applications, including probabilistic seismic hazard analysis, has been discussed in this deliverable. We here assesed and discussed the difference in the uncertainty of U-Net's interpolation of IMs between station locations when data from multiple networks rather than a single network is used. The operation of the U-net architecture is studied, and the U-net is trained using only the KiK-net dataset as well as both the KiK-net and MeSO-net databases. The KiK-net stations have an average inter-station distance of 94 km and 65 stations are located within our study region, ie the Kanto basin. The MeSo-net network is much denser than the KiK-net, with an average inter-station distance of 2-3 km and 300 observation stations located entirely within the Kanto basin, hence the difference of considering a high dense network in training can be understood.

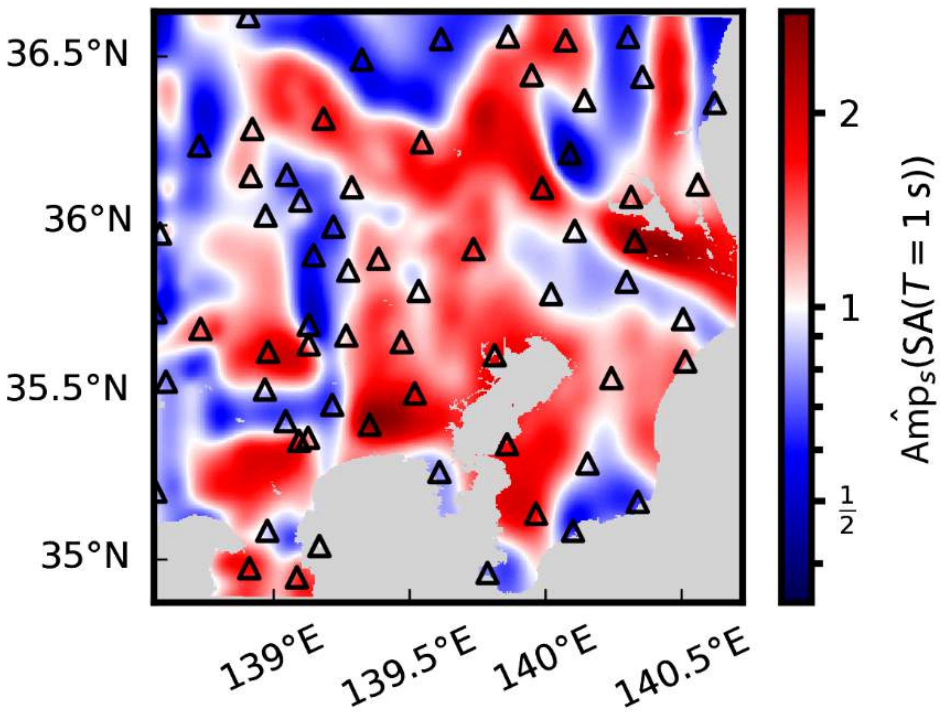

Figure 9: *Site amplication estimation of PSA at 1s in the Kanto basin approximated from averaged mean predictions using the KiK-net data. The black triangles indicate the station locations*

The U-net is trained using a single network and by integrating two networks within the same region while the validation stations remain the same. The partial ensemble predictions are analysed to understand the difference of prediction with and without including the MeSO-net. The rmse values between the observations and predictions of the partial ensemble estimators decreased after considering the dense network for training. The highest decrease in the rmse is found on the category of validation stations on validation events, which shows the effect of the new integrated network on the interpolation of U-Net, however the significance is still questionable as it is within the standard deviation. More dense networks are required to understand the significance of the decrease in the rmse values. We then compared the standardized residual distribution to analyse the accuracy of the predicted standard deviation. If the standard deviation is less than 1, it corresponds to overestimation of the uncertainty and vice-versa. Both the results show an overestimation of uncertainty by

14-15 %, however when we analysed the partial ensemble estimators the uncertainty range seems to decrease slightly and move towards one when both the datasets are used instead of only KiK-net. Although we integrated a spatially dense network along with the KiK-net dataset to compare the results, more networks with data quantity in both spatial and temporal scale is required to analyse and validate our results.

According to the results provided in this report, the error and the uncertainty tends to reduce with the integration of a spatially dense network, however more studies on the changes of IMs with spatial density is required. The site amplification in different frequencies is needed to be analysed and investigated using different seismological networks. The availability of the K-net data in the Kanto basin adds an advantage of another network availability within the same region. Integration of K-net along with the KiK-net and the MeSO-net will definitely improve the clarity of the results given in this report. Also, we have analysed the PGA values here, but it will be also more interesting and useful to examine the effect of integration of stations in higher periods PSA (T = 1s) because of its probabilistic seismic hazard analysis applications.

References

Aoi, S., Kimura, T., Ueno, T., Senna, S. & Azuma, H. (2021), 'Multi-data integration system to capture detailed strong ground motion in the tokyo metropolitan area', *Journal of Disaster Research* **16**(4), 684–699.

Bahrampouri, M., Rodriguez-Marek, A., Shahi, S. & Dawood, H. (2021), 'An updated database for ground motion parameters for kik-net records', *Earthquake Spectra* **37**(1), 505–522.

Blitzstein, J. K. & Hwang, J. (2015), *Introduction to probability*, Crc Press Boca Raton, FL.

Da, K. (2014), 'A method for stochastic optimization', *arXiv preprint arXiv:1412.6980* .

Douglas, J. (2020), 'Ground motion prediction equations 1964-2020'.

LeCun, Y., Bengio, Y. & Hinton, G. (2015), 'Deep learning', *nature* **521**(7553), 436–444.

Lilienkamp, H., von Specht, S., Weatherill, G., Caire, G. & Cotton, F. (2022), 'Ground-motion modeling as an image processing task: Introducing a neural network based, fully data-driven, and nonergodic approach', *Bulletin of the Seismological Society of America* **112**(3), 1565–1582.

NIED (2019), 'Nied f-net', *NIED* .

Ronneberger, O., Fischer, P. & Brox, T. (2015), U-net: Convolutional networks for biomedical image segmentation, *in* 'International Conference on Medical image computing and computer-assisted intervention', Springer, pp. 234–241.

Rumelhart, D. E., Hinton, G. E. & Williams, R. J. (1986), 'Learning representations by back-propagating errors', *nature* **323**(6088), 533–536.

Sakai, S. & Hirata, N. (2009), 'Distribution of the metropolitan seismic observation network', *Bull. Earthq. Res. Inst. Univ. Tokyo* **84**, 57–69.

Strasser, F. O., Abrahamson, N. A. & Bommer, J. J. (2009), 'Sigma: Issues, insights, and challenges', *Seismological Research Letters* **80**(1), 40–56.

Zerva, A. & Zervas, V. (2002), 'Spatial variation of seismic ground motions: an overview', *Appl. Mech. Rev.* **55**(3), 271–297.